Part II

- Use of Track Detectors for Momentum Measurement

- Gas Detectors
  - Proportional Chamber
  - Drift Chamber
  - TPC
  - MSGC, RPC, GEM

- Solid State Detectors
  - Strip Detectors
  - Pixel Detectors

→ R. Klanner, Friday, Sem 4

Momentum Measurement in B Field

Momentum is determined by measurement of track curvature $\kappa = 1/\rho$ in B field:

Measure sagitta s of the track. For the momentum component transverse to B field:

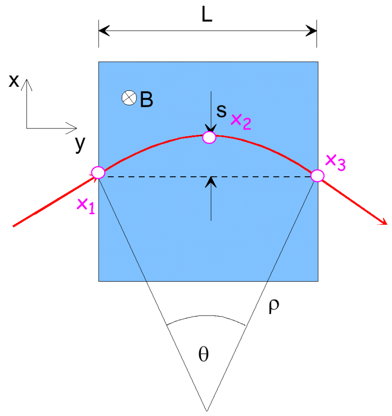

$$p_T = qB\rho$$

Units: $p_T[\mathrm{GeV}] = 0.3B[\mathrm{T}]\rho[\mathrm{m}]$

$$\frac{L/2}{\rho} = \sin\frac{\theta}{2} \approx \frac{\theta}{2} \text{ (for small } \theta) \Rightarrow \theta \approx \frac{L}{\rho} = \frac{0.3B\cdot L}{p_T}$$

$$s = \rho\left(1-\cos\frac{\theta}{2}\right) \approx \rho\left(1-\left(1-\frac{1}{2}\frac{\theta^2}{4}\right)\right) = \rho\frac{\theta^2}{8} \approx \frac{0.3L^2B}{8\;p_T}$$

For the simple case of three measurements:

$s = x_2-(x_1+x_3)/2 \Rightarrow ds = dx_2 - dx_1/2 - dx_3/2$

with $\sigma_x \approx dx_i$ uncorrelated error of single measurement:

$$\sigma_s^2 = \sigma_x^2 + \frac{\sigma_x^2}{4}\cdot 2 = \frac{3}{2}\sigma_x^2$$

Relative Momentum Error

For 3 points the relative momentum resolution is given by: $\frac{\sigma(p_T)}{p_T} = \frac{\sigma_s}{s} = \sqrt{\frac{3}{2}}\sigma_x \cdot \frac{8p_T}{0.3BL^2}$

- degrades linearly with transverse momentum
- improves linearly with increasing B field
- improves quadratically with radial extension of detector

In the case of N equidistant measurements according to Gluckstern [NIM 24 (1963) 381]:

$$\frac{\sigma(p_T)}{p_T} = \frac{\sigma(\kappa)}{\kappa} = \frac{\sigma_x\cdot p_T}{0.3BL^2}\sqrt{\frac{720}{(N+4)}}$$

(for $N \geq 10$, curvature $\kappa = 1/\rho$)

Example: For $p_T = 1\mathrm{GeV}$, $L = 1\mathrm{m}$, $B = 1\mathrm{T}$, $\sigma_x = 200\mu\mathrm{m}$ and $N = 10$ one obtains:

$$\frac{\sigma(p_T)}{p_T} \approx 0.5\% \quad \text{for a sagitta} \quad s \approx 3.8\mathrm{cm}$$

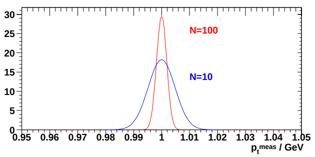

Important track detector parameter: $\frac{\sigma(p_T)}{p_T^2}$ (%/GeV)

Contribution from Multiple Scattering

The contribution to the momentum error from MS is given by:

$$\left.\frac{\sigma(p_T)}{p_T}\right|_{MS} = \frac{\sigma^{MS}(s)}{s} = \frac{\frac{L'}{\sqrt{3}}\frac{13.6\times10^{-3}}{p\beta}z\sqrt{\frac{L'}{X_0}}}{0.3BL^2z/(8p_T)} = \frac{0.2}{\beta B\sqrt{LX_0\sin\theta}}$$

with $L' = L/\sin\theta$ total path, $p_T = p\sin\theta$

for $\beta \to 1$ this part is momentum independent !

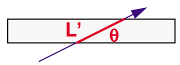

The combined total momentum error is:

$$\left(\frac{\sigma_p}{p}\right)^2 = \left(\sqrt{\frac{720}{N+4}}\frac{\sigma_x\,p\sin\theta}{0.3BL^2}\right)^2 + \left(\frac{0.2}{\beta B\sqrt{LX_0\sin\theta}}\right)^2 + (\cot\theta\sigma_\theta)^2$$

Example for momentum dependence of individual contributions

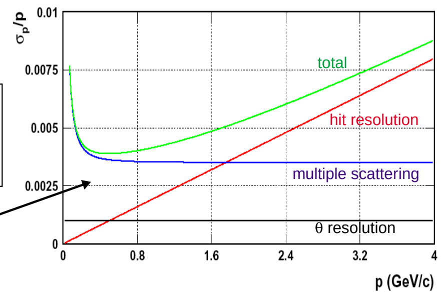

First Track Detectors

Until ≈ 1970:

- optical measurements using
  - bubble chambers
  - emulsions
  - spark chambers
- manual reconstruction
- can handle only very low data rates

BEBC bubble chamber

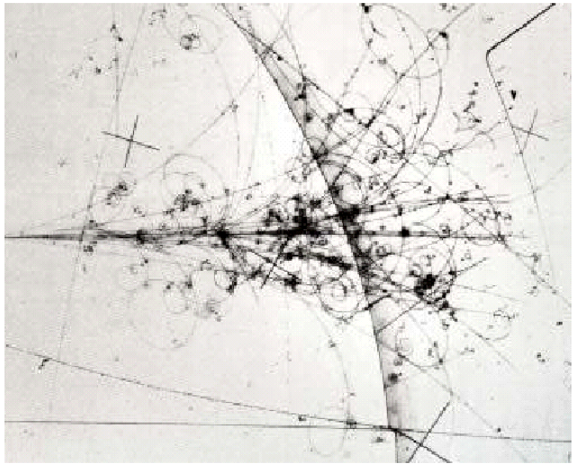

Gas Detectors

Criteria for optimal momentum resolution:

- many measurement points
- large detector volume
- very good single point resolution
- as little multiple scattering as possible

Gas detectors provide a good compromise and are used in most experiments. However:

- per cm in Argon only ca. 100 electron-ion pairs are produced by ionisation (see next page)
- this has to be compared with the noise of a typical amplifier of ≈1000 e-

⇒ a very efficient amplification mechanism is required

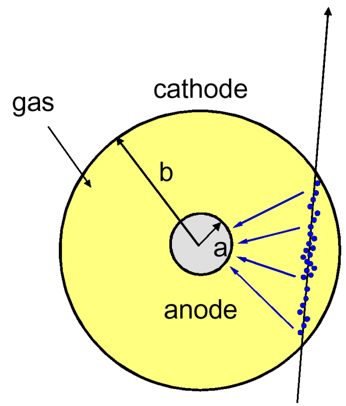

Primary and Total Ionisation Yield in Gases

Gas	Density ρ [g/cm^3]	I_0 [eV]	W [eV]	n_p [cm^{-1}]	n_T [cm^{-1}]
H_2	8.99 x 10^{-5}	15.4	37	5.2	9.2
He	1.78 x 10^{-4}	24.6	41	5.9	7.8
N_2	1.23 x 10^{-3}	15.5	35	10	56
O_2	1.43 x 10^{-3}	12.2	31	22	73
Ne	9.00 x 10^{-4}	21.6	36	12	39
Ar	1.78 x 10^{-3}	15.8	26	29	94
Kr	3.74 x 10^{-3}	14.0	24	22	192
Xe	5.89 x 10^{-3}	12.1	22	44	307
CO_2	1.98 x 10^{-3}	13.7	33	34	91
CH_4	7.17 x 10^{-4}	13.1	28	16	53
C_4H_{10}	2.67 x 10^{-3}	10.8	23	46	195

avg. ionisation pot. / shell elect.
average energy loss./ion pair
number primary electron-ion pairs
total number electron-ion pairs

@ STP

Total number of produced electron-ion pairs: $n_T = \frac{\Delta E}{W_i} = \frac{\frac{dE}{dx}\Delta x}{W_i}$ with

- ΔE = total energy loss in Δx and
- W_i = average energy loss per **produced** ion pair: $n_T \approx 2 \ldots 7 \cdot n_p$

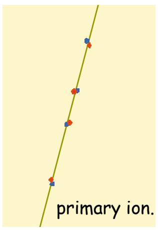

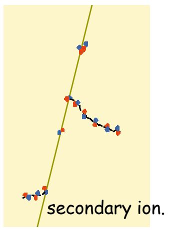

Gas Amplification

For cylindrical geometry:

$E(r) \propto \frac{1}{r}$ and $V(r) \propto \ln\frac{r}{a}$

- the primary electrons drift towards the positive anode
- due to 1/r dependence the electric field close to very thin wires reaches values of E > kV/cm
- ⇒ in between collisions with atoms electrons gain enough energy to ionize further gas molecules
- ⇒ exponential increase in number of electron-ion pairs very close (few µm) to the wire

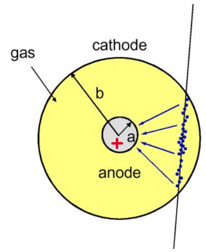

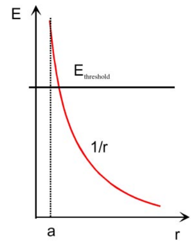

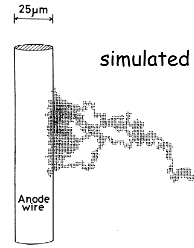

simulated avalanche

First Townsend Coefficient

Number of electron-ion pairs created per unit length in the avalanche per electron is given by the first Townsend coefficient α :

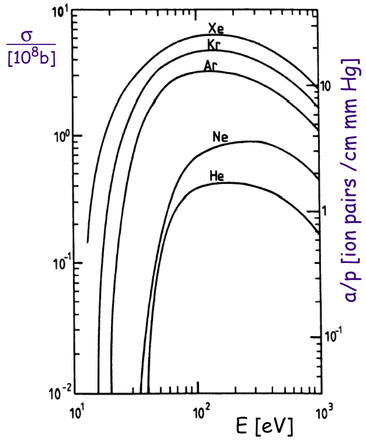

- relation to cross section for ionisation:

$$\alpha = \sigma_{ion} \cdot \frac{N_A}{V_{Mol}}$$

- number of produced ions: $n(x) = n_0 \cdot \exp(\alpha(E) \cdot x)$

- the gas gain is given by:

$$A = \frac{n}{n_0} = \exp\left[\int_a^{r_c} \alpha(r) dr\right]$$

  with a anode diameter and r_c distance to wire where avalanche starts

- example: Argon and E = 100eV: $\sigma = 3\text{x}10^{-16}\text{cm}^2 \Rightarrow \alpha^{-1} \approx 1\mu\text{m}$

Drift and Diffusion in Gas

No electric field (E = 0): thermal diffusion

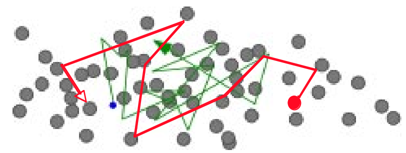

With electric field (E > 0): charge transport and diffusion

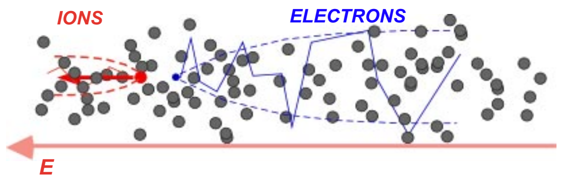

Avalanche Formation

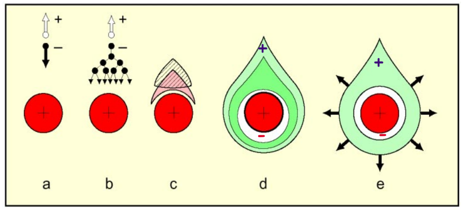

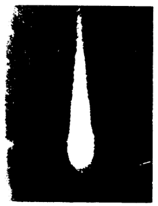

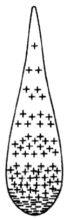

picture taken with cloud chamber

- due to transverse diffusion a droplet like avalanche develops around the anode
- electrons are collected very fast (≈ 1 ns) mobility of electrons ≈1000 times larger than for ions
- the cloud of positive ions remains and slowly drifts towards the cathode

Signal Shape

The signals which are induced on anode and cathode come from the fact that charges move in the electric field between the electrodes: $dv = \frac{Q}{lCV_0} \frac{dV}{dr} \cdot dr$

Most of the electron-ion pairs are created very close to the anode wire ⇒

- electrons only move a short distance in the electric field: dr small
- in contrast the ions move all the way back to the cathode: dr much larger
- ⇒ most of the signal is induced by the movement of the ions which takes ralativey long
- usually the signal has to be electronically differentiated

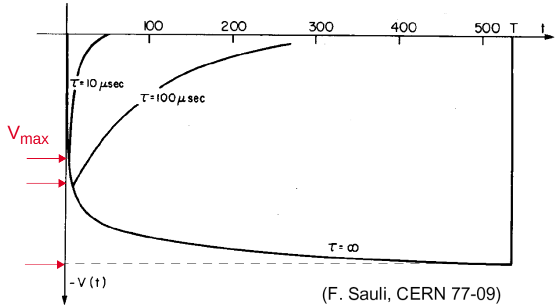

(F. Sauli, CERN 77-09)

Modes of Operation of Gas Detectors

- Ionisation chamber:
  complete charge collection, but no charge amplification.
- Proportional counter:
  above threshold voltage multiplication starts. Detected signal proportional to original ionization → energy measurement (dE/dx) possible. Secondary avalanches have to be quenched. Gain $\approx 10^4$-10^5
- Region of limited proportionality:
  or streamer mode: strong photo emission→ secundary avalanches. Needs efficient quencher or pulsed HV. Gain upto $\approx 10^9$, hence simple electronics sufficient.
- Geiger-Müller counter:
  massive photo emission. Full length of anode wire affected. Stop discharge by HV break down. Strong quenchers needed.

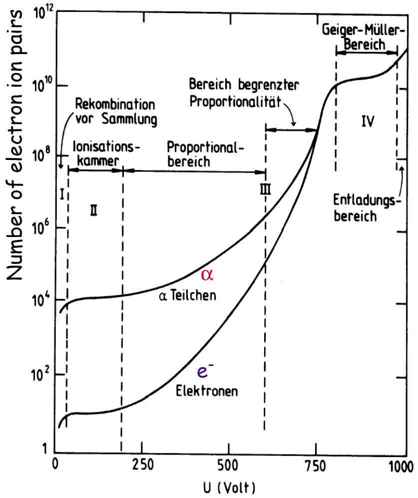

Family Tree of Gaseous Detectors

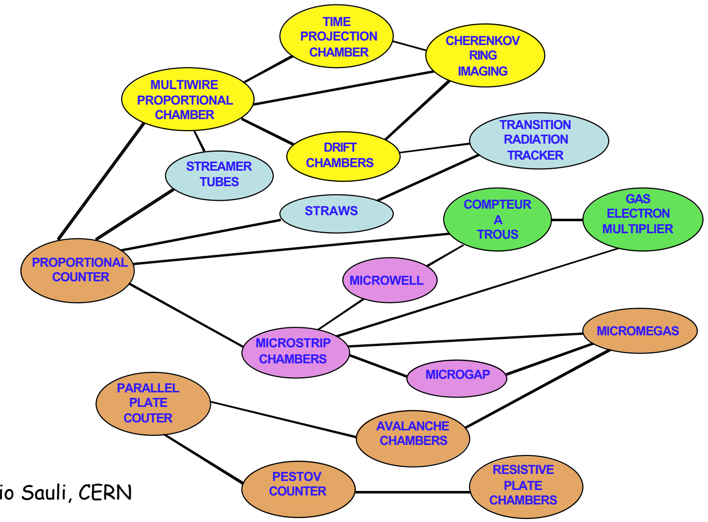

Fabio Sauli, CERN

Multi Wire Proportional Chamber

Generalize principal of proportional tube to large area detector.

Multi Wire Proportional Chamber: MWPC

George Charpak 1968

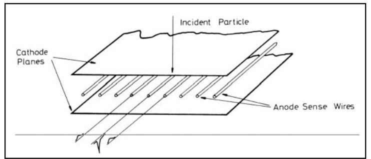

- anode wires act as independent detectors
- capacitive coupling of negative signal from anode wire where avalanche is formed to neighbours is small compared to pulse, which is generated by ions drifting towards cathode
- furthermore development in electronics: possibility to read many channels in parallel → 10^6 tracks per second

  ⇒ Breakthrough in detector development

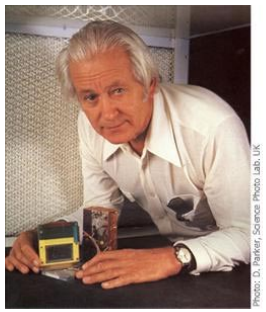

Nobelprize for physics 1992

MWPC

Use of gold plated tungsten wires with diameter 15-30µm as anode wires. Chamber walls made from glas fiber material (rigid, low mass). Thin metal foil acting as cathode (typically d≈50µm). Typical dimensions: d = 2mm, L = 4mm.

Electrostatic potential in a planar MWPC given by:

$$V(x,y) = -\frac{q}{4\pi\varepsilon_0}\ln\left\{4\left[\sin^2\left(\frac{\pi x}{d}\right)+\sinh^2\left(\frac{\pi y}{d}\right)\right]\right\}$$

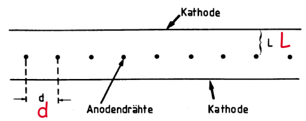

resolution σ = d/√12

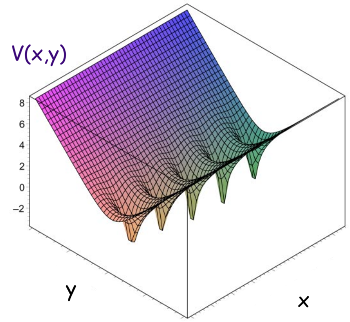

electric field lines

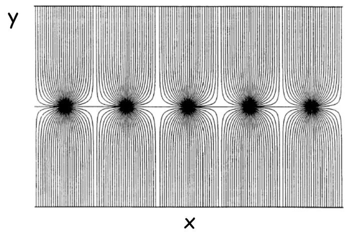

Principal of a Driftchamber

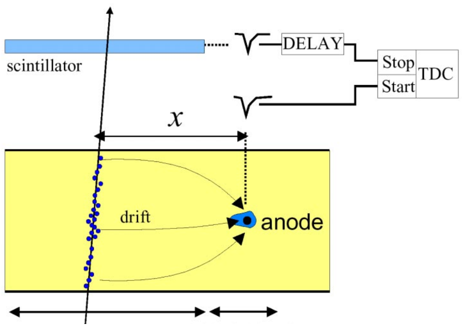

E-field small
drift region

E-field large
gas gain

TDC: Time to Digital Converter

Measure arrival time t_1 of electrons at anode wire relative to reference t_0.

- external definition of time reference t_0 (here by fast scintillator signal)
- x-coordinate given by:

$$x = \int_{t_0}^{t_1} v_D(t)dt$$

- if drift velocity v_D constant over full drift distance: $x = v_D(t_1 - t_0) = v_D \Delta t$
- advantage of drift chambers: much larger sensitive volume per read out channel

v_{drift} vs E-Field in various Argon-Mixtures

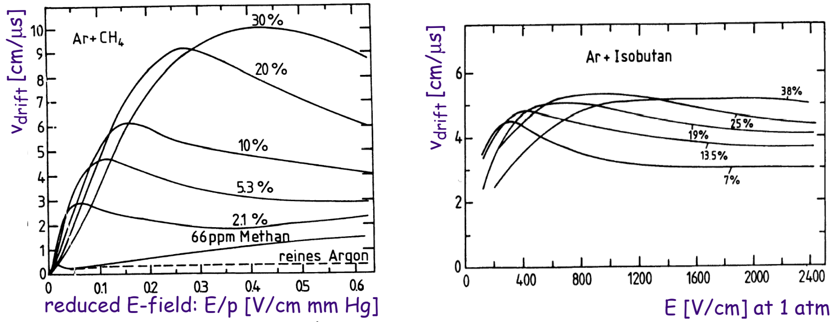

- strong dependence on the choice of the gas mixture
- details of the energy dependence of the ionisation cross section (Ramsauer minimum) result in a characteristic maximum of the E field dependence.
- for stable operation it is useful to operate in the maximum: $\frac{dv_{drift}}{dE} = 0$
- typical drift velocities : $v_{drift} \approx$ 2-10 cm/µs = 20-100 µm/ns

Examples for Cylindrical Driftchamber Geometries

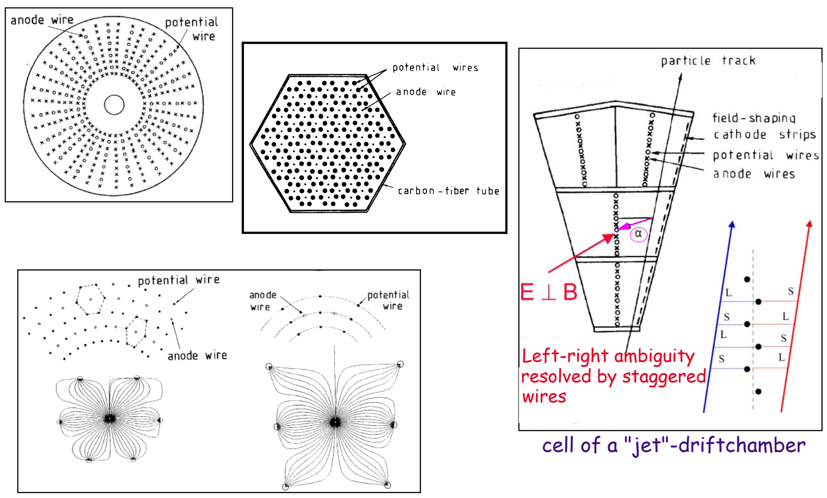

cell of a "jet"-driftchamber

Isochrones & Lorentzangle

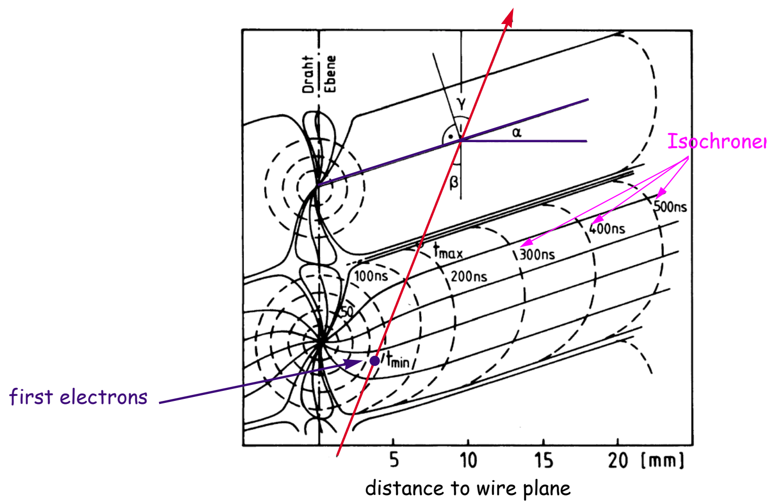

Intrinsic Position Resolution

The intrinsic position resolution is influenced by three effects:

- statistics of primary ionisation: point of origin of primary cluster varies by ≈100µm
- diffusion of electron cloud during it's drift to anode
  - $\sigma = \frac{1}{\sqrt{n}}\sqrt{\frac{2Dx}{\mu E}}$
  - Lorentz effect
- limitations in time resolution of whole chain of electronic signal processing
  - cabel
  - pulse shaping
  - definition of time refernce t_0 etc

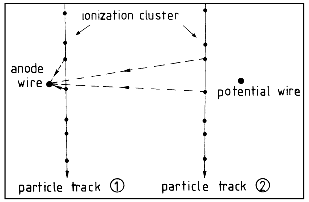

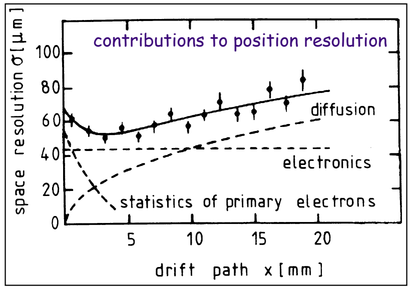

Driftchambers during Construction

H1 Central Jet Chamber

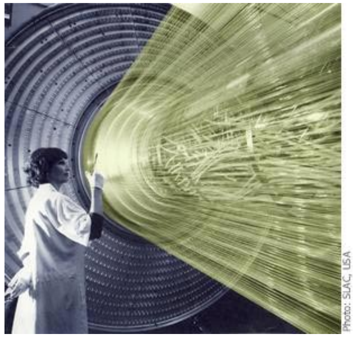

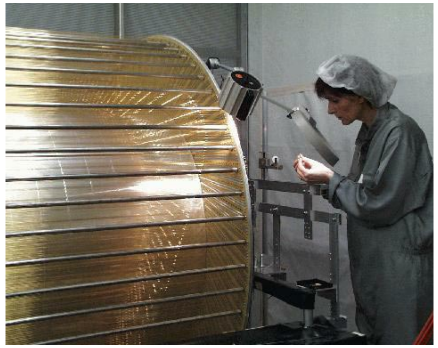

- ≈ 15000 wires
- total force from wire tension ≈ 6 tons

Options for Readout of Second Coordinate

Crossed Planes

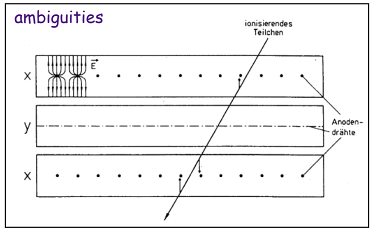

Charge Divison, z-by-timing

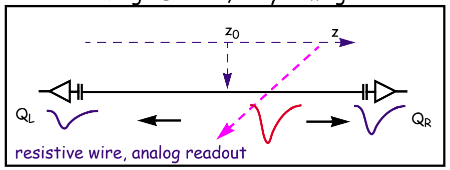

Segmented Cathodes

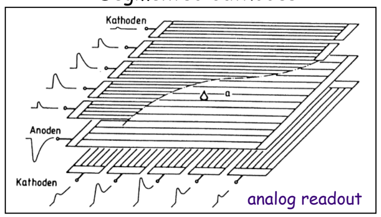

Stereo Wires

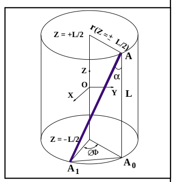

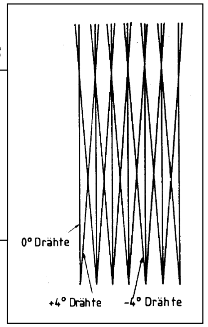

$\rightarrow \sigma_z \approx 0.1$ mm

Time Projection Chamber

In the seventies D.Nygren developed the Time Projection Chamber (TPC).

- large gas volume with one central electrode
- minimal amount of material
- electrons drift in strong electric field over distance of several meters to end walls where they can be registered for example with MWPCs
  - readout of anode wires and cathode pads → x,y
  - drift time → z
  - ⇒ unambiguous 3d hit measurements
- diffusion strongly reduced, since E || B ⇒ electrons spiral around E-field lines: Larmor radius <1µm
- laser calibration for precise v_D determination
- very good hit resolution and dE/dx meas.
- long drift times (≈40µs) ⇒
  - rate limitation
  - very good gas quality required

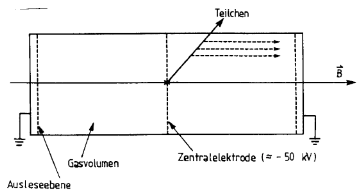

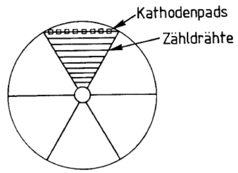

Example ALEPH TPC at LEP

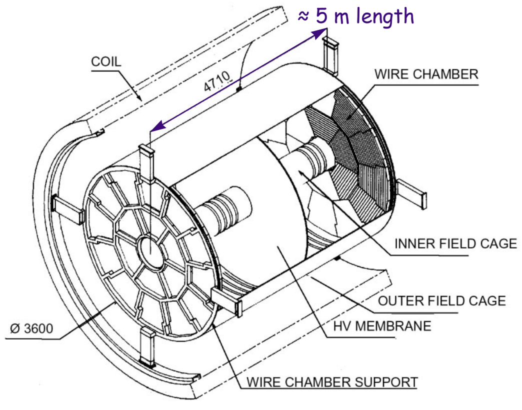

achieved resolutions:

$\sigma_{r\phi}$ = 170 μm

σ_z = 740 μm

r–φ projection

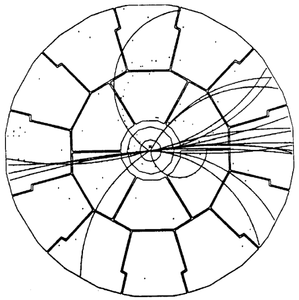

ALEPH TPC Event

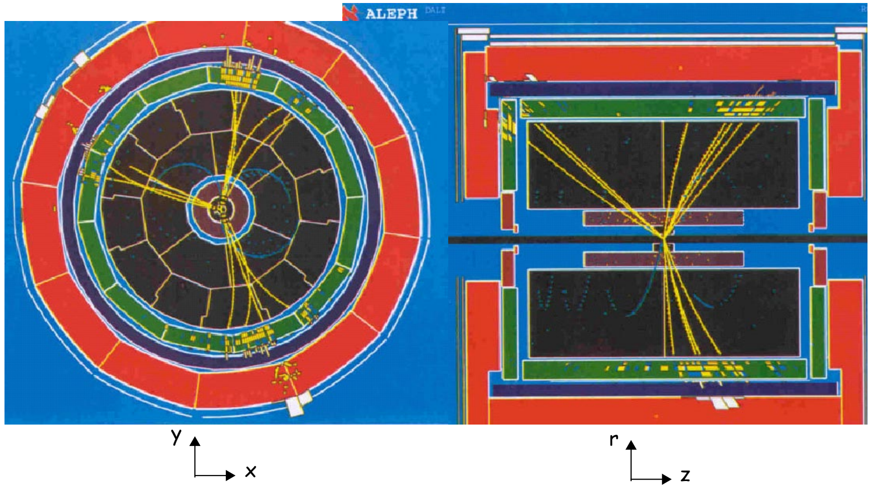

Example ALICE TPC @ LHC

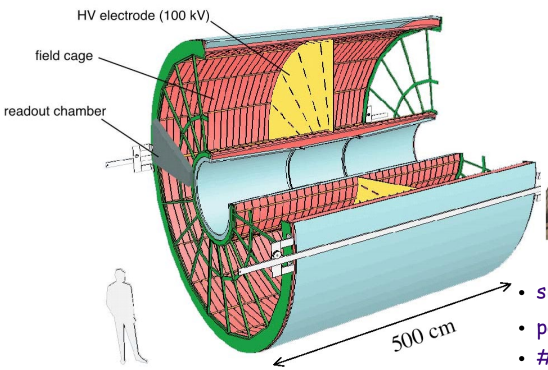

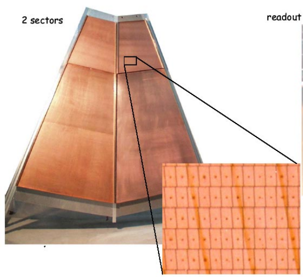

- size: L=5m, R=2.5m, V=88m^3
- pad size: 4 x 7.5 mm^2
- # channels: 570.000
- gas: Ne-CO_2 90:10
- gain: 2x10^4
- drift voltage: 100kV , 400V/cm
- start of operation: 2007

Construction of ALICE Field Cage

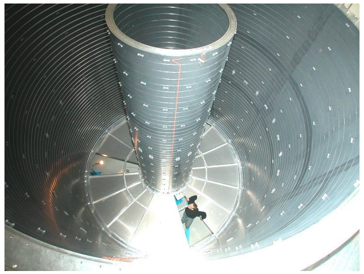

Gating in a TPC

A specific problem in a TPC is presented by the ions drifting back to the central electrode. At high rates they disturbe the homogeneity of the electric field in the drift region. Solution by so-called gating :

- ions are collected on shielding grid
- only electrons from "interesting" tracks reach the amplification region; others are collected on gating grid
- this requires use of an external trigger

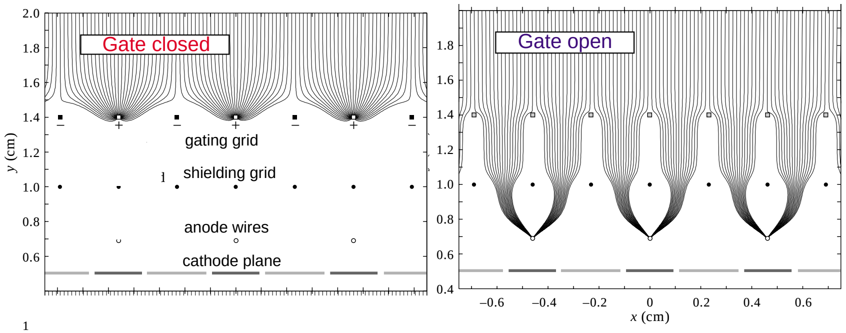

Aging Effects in Wire Chambers

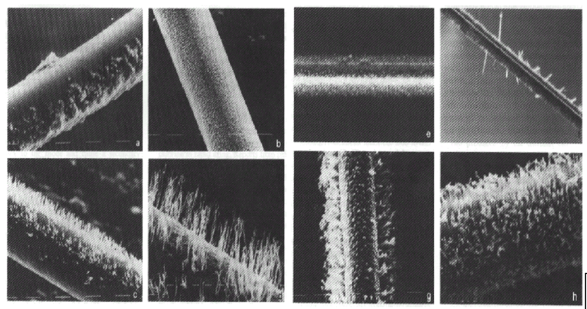

Deposits on anodes or cathodes.

Complex plasma-chemical reactions in the avalanche can lead to polymerisation.

This can make chambers completely unusable :

- inefficiency
- HV instabilities

Measures against aging:

- carefully selection of materials for whole system
- highest gas quality - no impurities
- avoid excessive chamber currents

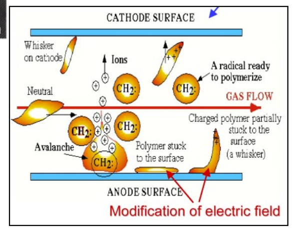

Micro Strip Gas Chambers MSGC

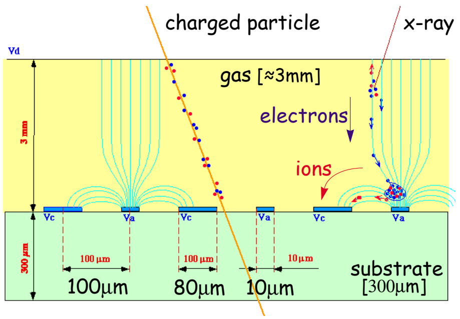

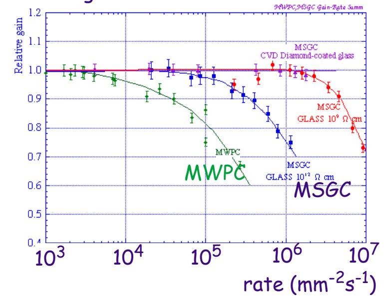

Advantages

- very precise and small anode/cathode structures can be produced with lithographical methods → very good position resolution
- high mechanical stability
- small drift distance for ions → high rate capability

Resistive Plate Chambers RPC

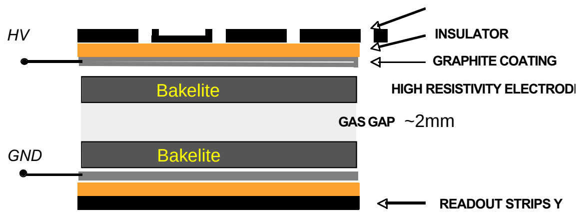

- robust and simple detector
  - no wires
- relatively cheap
  - well suited for large areas (muon systems)
- fast signal
  - < 5 ns (trigger)
- good rate capability
  - few kHz/cm^2

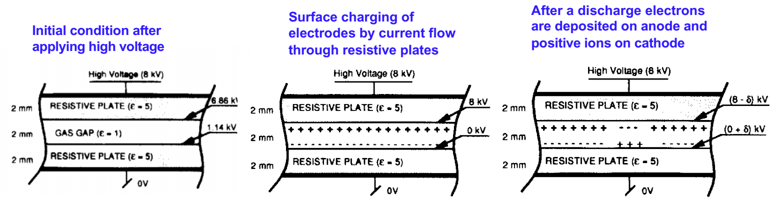

Gas Electron Multiplier GEM

In the late 90's developed by F.Sauli at CERN [NIM A386 (1997), 531]

- typical gain of $\approx 10^3$ at 500V
- can stack several stages on top af each other
- $\rightarrow$ large total gain at relatively moderate HV

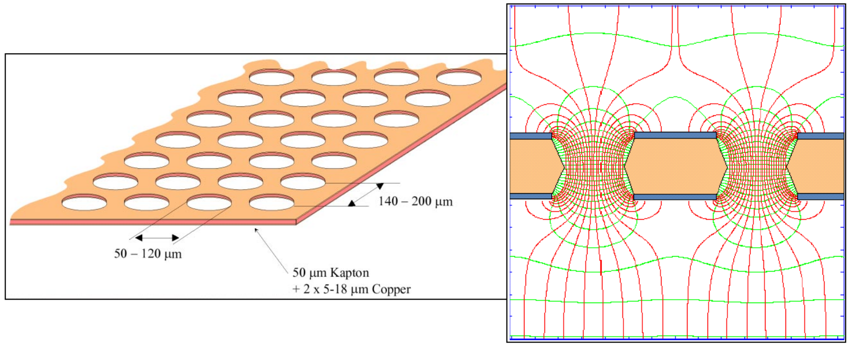

Main Characteristics of GEM Detectors

- Rate capability ~ 1 MHz mm^{-2}
- Position accuracy (MIPs) σ ~ 60 μm
- Radiation tolerance > 100 mC mm^{-2}
  - corresponds to ~ 10^{14} MIPs cm^{-2}

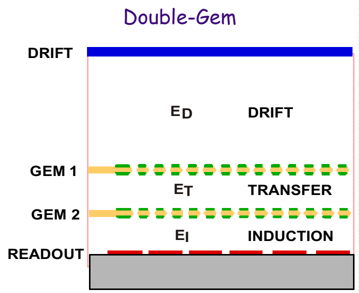

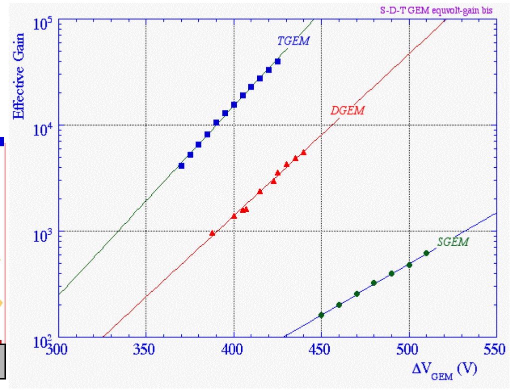

Detector R&D: GEM Readout for TPC at ILC

- Narrow pad response function: Δs ~ 1 mm
- Fast signals (no ion tail): Δt ~ 20 ns
- Very good multi-track resolution: ΔV ~ 1 mm^3
  - Standard MWPC TPC ~ 1 cm^3
- Ion feedback suppression: I+/I- ~ 0.1%

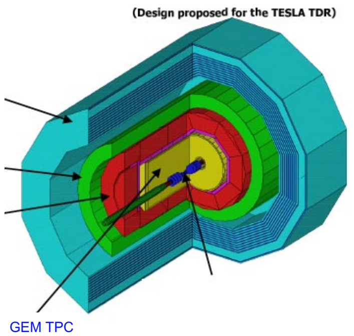

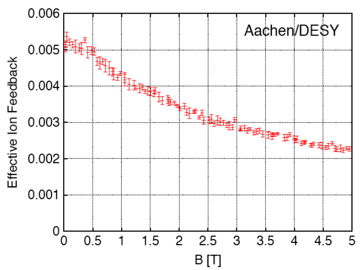

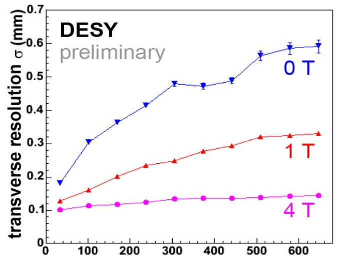

Summary on Track Detectors

- Relative momentum error of tracking device: $\left(\frac{\sigma_p}{p}\right)^2 \propto \left(a\frac{\sigma_x}{\sqrt{N}BL^2}p_T\right)^2 + \left(b\frac{1}{\beta B\sqrt{LX_0}}\right)^2$

  therefore need:
  - good hit resolution
  - large number of hits
  - large lever arm (size of detector)
  - large magnetic field
  - as little amount of dead material as possible (minimise multiple scattering at low momentum)
- Gas detectors
  - ionization $\rightarrow$ gas amplification process in high electric field yields detectable signal
  - wire chambers (MWPC, straws, drift chamber, TPC ...)
  - micro pattern devices (MSGC, GEM, Micromegas ...) for high rate applications
- Solid state detectors
  - mainly based on Silicon
  - micro structures (strips or pixels) provide excellent position resolution
  - for details see Friday lecture

Position and Timing Resolution

Detector Type	Accuracy (rms)	Resolution Time	Dead Time
Bubble chamber	10–150 μm	1 ms	50 ms[a]
Streamer chamber	300 μm	2 μs	100 ms
Proportional chamber	50–300 μm[b,c,d]	2 ns	200 ns
Drift chamber	50–300 μm	2 ns[e]	100 ns
Scintillator	—	100 ps/n[f]	10 ns
Emulsion	1 μm	—	—
Liquid Argon Drift [Ref. 6]	~175–450 μm	~ 200 ns	~ 2 μs
Gas Micro Strip [Ref. 7]	30–40 μm	< 10 ns	—
Resistive Plate chamber [Ref. 8]	$\lesssim$10 μm	1–2 ns	—
Silicon strip	pitch/(3 to 7)[g]	h	h
Silicon pixel	2 μm[i]	h	h

[a] Multiple pulsing time.
[b] 300 μm is for 1 mm pitch.
[c] Delay line cathode readout can give ±150 μm parallel to anode wire.
[d] wirespacing/$\sqrt{12}$.
[e] For two chambers.
[f] n = index of refraction.
[g] The highest resolution ("7") is obtained for small-pitch detectors ($\lesssim$25 μm) with pulse-height-weighted center finding.
[h] Limited by the readout electronics [9]. (Time resolution of $\leq$ 25 ns is planned for the ATLAS SCT.)
[i] Analog readout of 34 μm pitch, monolithic pixel detectors.

Semiconductors in the Periodic System

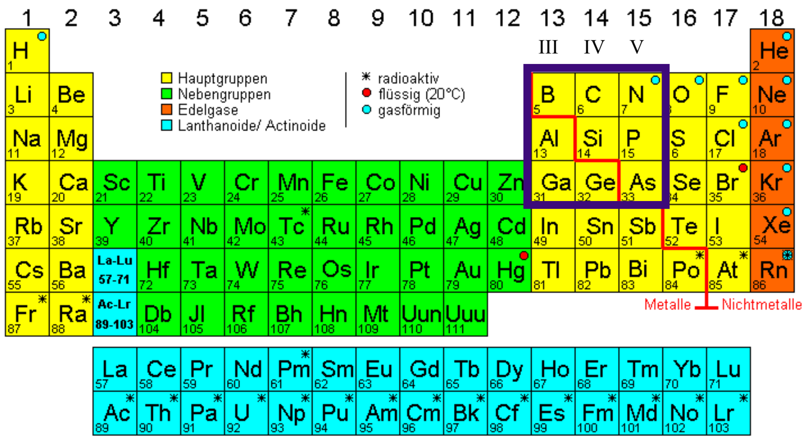

Advantages of Silicon

- band gap ΔE=1.12 eV
- energy needed per electron-hole pair: 3.6 eV (rest goes into phonons, for comparison ≈30eV for noble gas)
- high density: ρ = 2.33 g/cm^3
  with $dE/dx|_{min}$ = 1.664 MeV/gcm^{-2} one obtains for 300µm thick Si-layer:

  N = 300 µm x 1.664 MeV/gcm^{-2} x 2.33 g/cm^3 /3.6 eV

  ⇒ N ≈ 32000 electron-hole-pairs in 300 µm (MIP)
- good mechanical stability ⇒ layers of this thickness can be made self supporting
- large mobility of charge carriers ⇒ fast charge collection $\Delta t \approx$ 10ns
- no additional charge amplification mechanism neccessary